Exceptional Spin Liquids from Couplings to the Environment

Kang Yang,[1] Siddhardh C. Morampudi,[2] and Emil J. Bergholtz[1]
[1]*Department of Physics, Stockholm University, AlbaNova University Center, 106 91 Stockholm, Sweden*
[2]*Center for Theoretical Physics, Massachusetts Institute of Technology, Cambridge, Massachusetts 02139, USA*

(Received 14 July 2020; accepted 22 January 2021; published 16 February 2021)

We establish the appearance of a qualitatively new type of spin liquid with emergent exceptional points when coupling to the environment. We consider an open system of the Kitaev honeycomb model generically coupled to an external environment. In extended parameter regimes, the Dirac points of the emergent Majorana fermions from the original model are split into exceptional points with Fermi arcs connecting them. In glaring contrast to the original gapless phase of the honeycomb model that requires time-reversal symmetry, this new phase is stable against all perturbations. The system also displays a large sensitivity to boundary conditions resulting from the non-Hermitian skin effect with telltale experimental consequences. Our results point to the emergence of new classes of spin liquids in open systems that might be generically realized due to unavoidable couplings with the environment.

DOI: 10.1103/PhysRevLett.126.077201

Quantum spin liquids are low-temperature phases of matter with fractionalized excitations and emergent gauge fields [1–5]. Efforts at identifying possible spin liquids have led to hundreds of candidates due to the various possible symmetries present in lattice systems. However, a broader view of the nature of the fractionalized excitations and gauge field leads to only a few prominent types [2], some of which are realized in exactly solvable models [6–14]. Here, we show that coupling a spin liquid to an environment can lead to a qualitatively new kind of phase that cannot occur in any closed system.

Dissipative systems can display unusual phenomenology not seen in closed systems. These range from unusual phase transitions and critical phases [15–18] to new topological phases [19–22]. One prominent class of phenomena can be understood in regimes where a non-Hermitian description [19,20,23–28] of the system is appropriate. This allows for the appearance of exceptional points in the spectrum when two eigenvectors coincide [29–32]. In noninteracting systems, band crossings with such exceptional points result in an unconventional square-root dispersion at low energies as opposed to a typical Dirac dispersion as seen in graphene. These band crossings in two-dimensional (2D) systems are generic, unlike the accidental symmetry-protected crossings in graphene [19,22]. The conventional bulk-boundary correspondence is also shown to be broken due to an exotic non-Hermitian skin effect [33–40], which results in localization of all eigenstates at the boundary. This results in an exponential sensitivity of the system to boundary conditions. Based on work of free systems, interest is now drawn to understanding effects in interacting systems [16,41–46]. It is then natural to ask how the emergent phenomena in strongly correlated spin liquids look like when the system is described by such an effective non-Hermitian Hamiltonian.

In this Letter, we show that these phenomena can be realized in an interacting spin model, giving rise to a qualitatively new kind of spin liquid. We illustrate this by coupling the Kitaev honeycomb model [7] to an environment (Fig. 1, left panel). In certain regimes, the two Dirac points generically split into four exceptional points

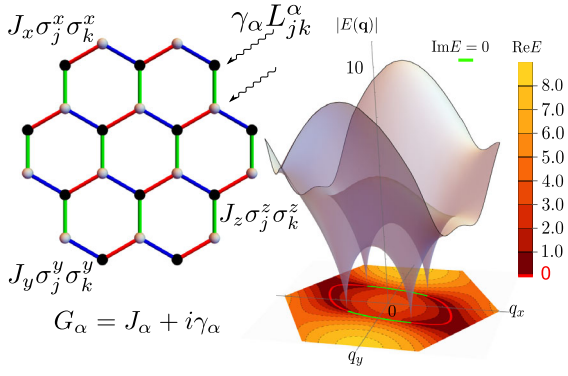

FIG. 1. Left: The lattice of the Kitaev honeycomb model. The spins are coupled through $J_\alpha\sigma_j^\alpha\sigma_k^\alpha(\alpha = x, y, z)$. The coupling to the environment is described by jump operators L_{jk}^α. Right: The three-dimensional (3D) spectrum diagram for the non-Hermitian Kitaev honeycomb model at $G_x = 2$, $G_y = 1$, $G_z = 2.5\exp(i\pi/3)$. The Fermi arc (Re$E = 0$) is labeled with the red line, and the green line indicates the Im$E = 0$ curve.

(Fig. 1, right panel). The four exceptional points are paired up, with each pair connected through Fermi arcs reminiscent to those found in Weyl semimetals [47] but occurring in the bulk rather than on the boundaries of the system. Unlike the closed system where the ferromagnetic spin liquid and the antiferromagnetic spin liquid are separated by a nodal-line critical point, the open system can go from one to the other by splitting and recombination of exceptional points. Moreover, the only way to produce a gap is to bring the exceptional points together: again, similar to Weyl points in 3D. Thus, the coupling to the environment elevates a symmetry-protected gapless spin liquid to a generically stable phase, which we term an *exceptional spin liquid*. We also show the occurrence of the skin effect on open zigzag boundaries leading to a large sensitivity on boundary conditions. Finally, we show that the phenomena are naturally expected to arise in potential realizations of the honeycomb model, such as those proposed in cold atoms and ion traps.

Model.—The Kitaev honeycomb model [7] is defined through compass interactions linking directions in spin space and real space of the spin 1/2:

$$H_0 = -\sum_{\langle jk\rangle_\alpha} J_\alpha \sigma_j^\alpha \sigma_k^\alpha, \tag{1}$$

where $\langle jk\rangle_\alpha$ labels the lattice (Fig. 1), and $\alpha = x, y, z$ labels the three types of links of a hexagonal lattice with σ^α as the corresponding Pauli matrices.

We consider an open system where the Kitaev Hamiltonian is coupled to an environment. The resulting open system is described by a Lindblad master equation [48] for the density matrix

$$\frac{d}{dt}\rho = -i[H_0, \rho] + \sum_{\langle jk\rangle_\alpha} \gamma_\alpha \left(L_{jk}^\alpha \rho L_{jk}^{\alpha\dagger} - \frac{1}{2}\{L_{jk}^{\alpha\dagger} L_{jk}^\alpha, \rho\} \right), \tag{2}$$

where L_{jk}^α are jump operators describing how the system is coupled to the bath, and we have set $\hbar = 1$. The dynamics can be interpreted in terms of deterministic evolution of a trajectory (wave function) described by an effective non-Hermitian Hamiltonian

$$H_{\mathrm{NH}} = H_0 - (i/2)\sum_{\langle jk\rangle_\alpha} \gamma_\alpha L_{jk}^{\alpha\dagger} L_{jk}^\alpha,$$

interspersed with quantum jumps to different states through the $L_{jk}^\alpha \rho L_{jk}^{\alpha\dagger}$ term [49–52]. Thus, when we are measuring at times before the first jump, the dynamics is governed by the non-Hermitian Hamiltonian H_{NH}. This can be interpreted as a measurement backaction in settings where realizations of the model system are postselected to consider only cases where the jump has not occurred [51–55].

Although the general phenomenology of what follows is largely independent of the form of the jump operators, we consider here jump operators $L_{jk}^\alpha = \sigma_j^\alpha + \sigma_k^\alpha$ along each α-type link $j-k$ for illustration. Similar results can be obtained by considering the effect of dephasing noise [56]. This results in an effective non-Hermitian description of the form of Eq. (1) but with the coupling constants being complex, and henceforth labeled by $G_\alpha = J_\alpha + i\gamma_\alpha$. This model is exactly solved through an enlarged Majorana representation of the spin operators. Introducing four Majorana fermions $(c_j, b_j^x, b_j^y, b_j^z)$ at each site, the spin is represented as $\sigma_j^\alpha = i c_j b_j^\alpha$. The physical state is constrained by the condition $D_j|\mathrm{phys}\rangle = |\mathrm{phys}\rangle$, with $D_j = b_j^x b_j^y b_j^z c_j$. Defining bond operators $u_{jk} = i b_j^\alpha b_k^\alpha$, where α is the type of link $j-k$, the effective model is

$$H_{\mathrm{NH}} = -\sum_{\langle jk\rangle_\alpha} G_\alpha \sigma_j^\alpha \sigma_k^\alpha = i\sum_{\langle jk\rangle_\alpha} G_\alpha u_{jk} c_j c_k. \tag{3}$$

The bond operator u_{jk} is a constant of motion in the enlarged Majorana representation. Meanwhile, a physical conserved quantity is the product of u_{jk} around a plaquette p,

$$W_p = \prod_{j-k\in p} u_{jk}.$$

The eigenvectors can thus be grouped into different sectors of the eigenvalues $W_p = \pm 1$. The sector with all $W_p = 1$ is viewed as vortex free, and $W_p = -1$ means a $\mathbb{Z}_2$ vortex at p.

The eigenstates of the model can be decomposed into different $\mathbb{Z}_2$-flux sectors as in the original Hermitian model, where the zero flux is the relevant one at low (real) energies due to Lieb's theorem [7,57]. In fact, the zero-flux sector is still relevant for the open systems in appropriate regimes where all the phenomenology we discuss is realized. To illustrate this, consider the Hermitian model at temperatures much lower than the vison gap. If we consider multiplying it by an overall complex number, there is a parametric separation in lifetimes of states between different flux sectors, and the zero-flux sector corresponds to states with the longest lifetimes. In the Supplemental Material, we provide numerical evidence that this also holds true in more general cases [58].

In the zero-flux sector, we can choose $u_{jk} = 1$ for j on one sublattice and k on the other. The Hamiltonian becomes a tight binding Majorana model in momentum space as

$$\tilde{H} = \sum_{\mathbf{q}}{}' \begin{pmatrix} c_{-\mathbf{q},1} c_{-\mathbf{q},2} \end{pmatrix} \begin{pmatrix} 0 & iA(\mathbf{q}) \\ -iA(-\mathbf{q}) & 0 \end{pmatrix} \begin{pmatrix} c_{\mathbf{q},1} \\ c_{\mathbf{q},2} \end{pmatrix}, \tag{4}$$

where in the primed summation

$$\sum{}',$$

we count the pair $\mathbf{q}, -\mathbf{q}$ only once. This is because $c_{-\mathbf{q}} = c_{\mathbf{q}}^{\dagger}$. The off-diagonal element is $A(\mathbf{q}) = 2(G_x e^{i\mathbf{q}\cdot\mathbf{r}_1} + G_y e^{i\mathbf{q}\cdot\mathbf{r}_2} + G_z)$, and the subscripts 1 and 2 label the two sublattices of the honeycomb system. The momentum-space operators satisfy $\{c_{\mathbf{q},\lambda}, c_{-\mathbf{q}',\gamma}\} = \delta_{\mathbf{q},\mathbf{q}'}\delta_{\lambda,\gamma}$. Depending on whether $A(\mathbf{q})$ can go to zero, the system exhibits a gapped or a gapless phase. In the Hermitian model, the gapped phase is equivalent to a toric code spin liquid [6], whereas the gapless phase can possess non-Abelian statistics in the presence of a magnetic field [7]. The gapless condition is given that the lengths $|G_x|$, $|G_y|$, and $|G_z|$ admit a triangle:

$$|G_x| \le |G_y| + |G_z|, |G_y| \le |G_x| + |G_z|, |G_z| \le |G_x| + |G_y|. \tag{5}$$

Exceptional points and Fermi arcs.—The spectrum is obtained by the eigenvectors of the matrix [Eq. (4)]: $E^2(\mathbf{q}) = A(\mathbf{q})A(-\mathbf{q})$. In the Hermitian case, there are two Dirac points inside the gapless region. We show that for complex G_α, the band-touching points have a square-root dispersion and are exceptional points.

For convenience of computation here, we can extract out the phase of G_z as an overall phase of $\tilde{H}$, and so the Hamiltonian is now parameterized by $\bar{\phi}_x = \phi_x - \phi_z$ and $\bar{\phi}_y = \phi_y - \phi_z$. In the Brillouin zone, it is more convenient to parametrize as $\mathbf{q} = \mathbf{q}_1\tilde{q}_1/(2\pi) + \mathbf{q}_2\tilde{q}_2/(2\pi)$, where $\mathbf{q}_1$ and $\mathbf{q}_2$ are the reciprocal lattice vectors. The values $\tilde{q}_1$ and $\tilde{q}_2$ uniquely fix the vector $\mathbf{q}$ (notice that we should take $\tilde{q}_1$, $\tilde{q}_2$ mod 2π). Zero energy at $\mathbf{q}$ implies $A(\mathbf{q}) = 0$ or $A(-\mathbf{q}) = 0$. The $A(\mathbf{q}) = 0$ condition gives $\tilde{q}_1$ and $\tilde{q}_2$:

$$\tilde{q}_{1(2)} = \pm\cos^{-1}\left(\frac{|G_{y(x)}|^2 - |G_z|^2 - |G_{x(y)}|^2}{2|G_{x(y)}||G_z|}\right) - \bar{\phi}_{x(y)} \tag{6}$$

with the constraint $G_x \sin(\tilde{q}_1 + \bar{\phi}_x) = -G_y \sin(\tilde{q}_2 + \bar{\phi}_y)$ to fix the $\pm$ signs above. These equations admit, at most, two solutions; and we denote them as $\mathbf{q}_e$ and $\mathbf{q}'_e$. In the Hermitian situation, one has $A^*(\mathbf{q}) = A(-\mathbf{q})$ and $\mathbf{q}_e = -\mathbf{q}'_e$ as $\bar{\phi}_x = \bar{\phi}_y = 0$. Linearizing A, it directly follows that we have Dirac points with a conventional linear dispersion away from the degeneracies.

For complex (i.e., non-Hermitian) parameters, we have $A^*(\mathbf{q}) \neq A(-\mathbf{q})$ and $\mathbf{q}_e = -\mathbf{q}'_e - 2(\bar{\phi}_x, \bar{\phi}_y)$. Now, $A(\mathbf{q})$ and $A(-\mathbf{q})$ vanish at different points, implying four $E = 0$ exceptional points $\pm\mathbf{q}_e$ and $\pm\mathbf{q}'_e$ at which the Hamiltonian matrix becomes nondiagonalizable and the two eigenvectors coincide. The dispersion near the exceptional points takes a square-root form instead of the conic form since $A(\mathbf{q})$ and $A(-\mathbf{q})$ do not vanish simultaneously. The $\mathrm{Re}E = 0$ branch cuts associated with the square roots have a natural interpretation as bulk Fermi arcs, and the exceptional points are connected by these Fermi arcs and their imaginary counterparts $\mathrm{Im}E = 0$ (cf. Fig. 1, right panel).

When the coupling constants are tuned out of the triangle regime [Eq. (5)], the four exceptional points fuse into two exceptional points and then disappear. A cut at $G_x = 2$ and $G_y = 1$ for different complex G_z is shown in Fig. 2, where we also plot the absolute energy $|E|$ and its real part $\mathrm{Re}E$ at different G_z. One can see the splitting of each Hermitian band-touching point into two non-Hermitian exceptional points. At the phase boundary, the branch cut for E disappears. In this situation, the band-touching point is

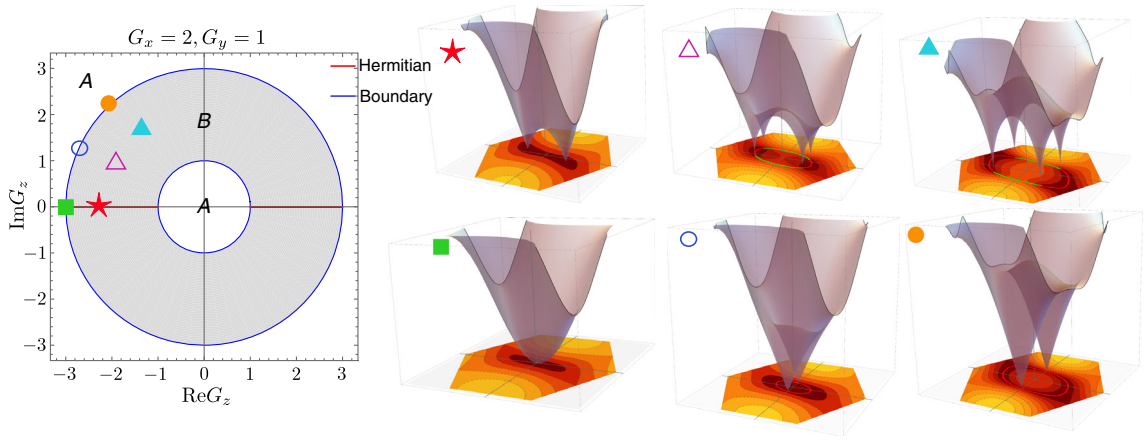

FIG. 2. The spectrum and phase diagram for the non-Hermitian Kitaev honeycomb model at $G_x = 2$, $G_y = 1$. The gray region B admits band-touching points, whereas region A possesses a (complex) gap. Six values of G_z are taken to exhibit different dispersions with respect to $\mathbf{q}$ as in Fig. 1. For the Hermitian situation (the star), around the band-touching point, $E \sim \sqrt{g_{\alpha\beta}\delta q_\alpha \delta q_\beta}$ with coefficients $g_{\alpha\beta}$. At the Hermitian phase boundary (the square), the dispersion is quadratic along a certain direction $E \sim \sqrt{(g_\alpha \delta q_\alpha)^4}$ with coefficients g_α. In the non-Hermitian situation (the two triangles), the dispersion is square-root $E \sim \sqrt{g'_\alpha \delta q_\alpha}$. At the non-Hermitian boundary (the two circles), the energy is linear along some direction $E \sim \sqrt{g'_{\alpha\beta}\delta q_\alpha \delta q_\beta}$.

not protected, and thus gets gapped out when crossing the phase boundary. This illustrates how, similar to Weyl points in 3D, the exceptional points can only be gapped out when combined pairwise, which is in glaring contrast to the 2D Dirac points that are inherently symmetry protected.

Skin effects.—Boundary conditions do not affect the spectrum for Hermitian systems in the thermodynamic limit, except for additional edge states. In contrast, non-Hermitian systems display a strong sensitivity to boundary conditions. To illustrate this, we consider Eq. (3) with two parallel zigzag boundaries. We place the open boundary condition perpendicular to the z-type link, which is along the y direction. The x direction is still chosen to be periodic with N_x unit cells. For convenience of comparison with the periodic boundary condition (PBC), the number of layers sandwiched by the two boundaries is taken to be even $M = 4M'$. The Hamiltonian is diagonal in the momentum q_x, and we denote the state by $\psi(m)$ with m as the layer index. The boundary conditions require $\psi(0) = 0$ and $\psi(M+1) = 0$. The question can be solved by a transfer matrix method [58,59]. We group the wave functions into a doublet $\Psi(m) = [\psi(2m), \psi(2m+1)]$. Then, the equation of motion takes the form $\Psi(m) = T\Psi(m-1)$, where T is the transfer matrix (details in [58]). Each eigenstate $\Psi(m)$ can be therefore constructed as a superposition of the two eigenvectors of T, $\Psi(m) = \alpha s_1^m \Psi_1 + \beta s_2^m \Psi_2$, with $\Psi_{1,2}$ as the eigenvectors of T and $s_{1,2}$ as the corresponding eigenvalues, such that it satisfies $\psi(0) = \psi(M+1) = 0$. If we consider Hermitian couplings, then $|s_1| = |s_2| = 1$ and the eigenstates propagate into the bulk. However, in the non-Hermitian situation, $s_1 \simeq s_2$ are either both larger or smaller than one, and the states are piled up against one of the boundaries. These are known as the non-Hermitian skin effects [33,34]. The general criterion for the skin effect is when $|s_1 s_2|$ is given by

$$|\det T| = \frac{|G_x e^{iq_x a} + G_y|}{|G_x e^{-iq_x a} + G_y|} \neq 1. \tag{7}$$

In this case, all eigenstates are exponentially localized to the boundary $\psi(m) \sim \exp(-m/l)$, with $l = (\ln|\det T|)/2$. We see that this occurs when the relative phase $\phi_x - \phi_y$ is nonzero. By rotation symmetry, we can draw the conclusion that for two parallel zigzag open boundaries perpendicular to α-type links, the skin effects can be turned on by giving a nontrivial relative phase $\phi_\beta - \phi_\gamma$, where $\beta, \gamma \neq \alpha$.

In Figs. 3(a)–3(c), we show the open-boundary-condition (OBC) spectra for different constants. The average localization of the wave function

$$\bar{m} = \sum m|\psi(m)|^2$$

is indicated with the color plot. For a nonvanishing $\phi_x - \phi_y$, as in Fig. 3(a), in addition to the zero-energy boundary state, the bulk states are also piling up the $m = 1$ boundary, exhibiting the skin effects. The localization shifts from one boundary to the other at $q_x = 0, \pi$, in accordance with Eq. (7). The spectrum is strikingly different from the PBC spectrum. For a vanishing $\phi_x - \phi_y$ and nonvanishing ϕ_z, we can, however, see in Fig. 3(b) that there is no skin effect despite the presence of bulk exceptional points; and the OBC spectrum coincides with the PBC spectrum. Figure 3(c) shows a Hermitian example contrasting with the novel non-Hermitian behaviour.

Discussion.—We have shown in this Letter that genuinely non-Hermitian phenomenology, exceptional points, and skin effects intriguingly conspire with fractionalization in the interacting Kitaev honeycomb model in dissipative environments. This results in a qualitatively new type of non-equilibrium matter that we call exceptional spin liquids, which by its dissipative nature lies beyond earlier classification schemes and potentially displays new dynamics beyond current spin liquids [60–63]. Remarkably, this new phase is generic in the sense that it does not rely on any underlying symmetries—this may in fact greatly facilitate the prospects for observing gapless spin liquids in synthetic setups.

The exceptional points can naturally arise in many of the proposed realizations of the Kitaev honeycomb model [64–69]. Two concrete mechanisms involve incorporating effects of a self-energy [70] and a postselection procedure [51,52,54,71] on synthetic realizations. The material

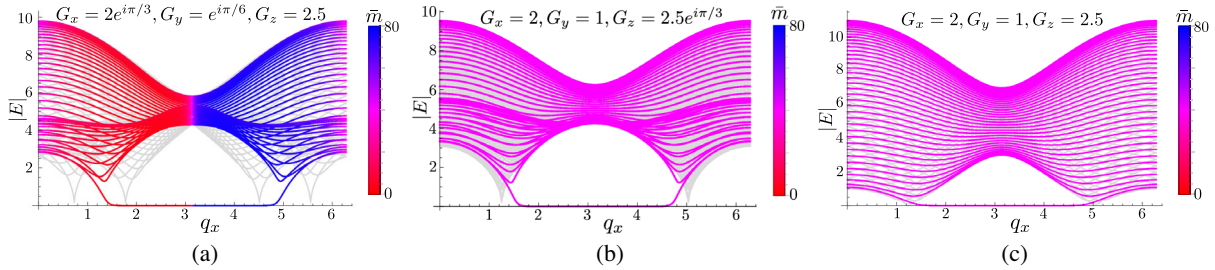

FIG. 3. The spectra of the system for OBC (colored) and PBC (light gray) as well as the corresponding average localization of the eigenstates. (a) A non-Hermitian skin effect occurring due to the nontrivial relative phase $\phi_x - \phi_y \neq 0 (\mathrm{mod}\, \pi)$. (b) The skin effect does not occur if only G_z is tuned complex while $\phi_x - \phi_y = 0 (\mathrm{mod}\, \pi)$. (c) The Hermitian case, where the PBC and OBC spectra overlap, except for the edge mode. All results are obtained for a $M = 80$-row lattice.

candidates for the Kitaev honeycomb model could potentially realize this non-Hermitian phenomenology if the effects of excitations such as phonons are taken into account. Here, we expound on the postselection procedure in a synthetic optical lattice system of ultracold atoms. Such systems are unavoidably subject to dissipative effects, most notably from spontaneous emission and inelastic collisions [72,73]. As mentioned above [Eq. (2)], the absence of quantum jumps from such processes leads to a measurement backaction [51–55] resulting in a non-Hermitian evolution. If spontaneous emission is the dominant dissipative mechanism, the procedure is implemented by a continuous measurement of the system to monitor for emitted photons and a postselection on those realizations where no photons are observed.

Considering ^{87}Rb atoms with a typical magnetic scale of 100 Hz, the scattering rate due to spontaneous emission is a few hertz. It is dependent on the detuning Δ of the laser as Δ^{-2}, and can hence be tuned appropriately across a wide range from milliseconds to many minutes [74]. Further tuning can be achieved by using different transitions in the same or different atoms since the spontaneous emission rate goes as ω_0^3, where ω_0 is the transition energy. The losses due to inelastic collisions can also be tuned through techniques such as external confinement, Feshbach resonance, and photoassociation [72]. The Kitaev honeycomb model can be realized with hyperfine states and a spin-dependent potential [64]. Using different detunings for the different lasers creating the lattice can then result in the direction-dependent Lindblad operators necessary for the phenomenology here. Although it would seem beneficial to have a detuning that is as large as possible, since that would lead to a bigger separation of the exceptional points, it is practically limited by the transition frequency. More importantly, it also makes the postselection procedure more difficult since the Poissonian decay process means that the probability of a decay not occurring would be $\sim e^{-N\gamma/\delta}$, where γ is the noise rate, N is the number of spins, and δ is the imaginary part of the many-body gap. Hence, the primary challenge would be to resolve the exceptional points due to a small separation. Choosing parameters such that the zero-flux sector has the longest lifetime (see Supplemental Material [58]) would give an enhancement to the naive lifetime and might allow one to choose larger noise rates to better resolve the exceptional points.

The exquisite control and ubiquitous presence of dissipation in the suggested synthetic implementations of our ideas might even open the door for novel technological applications such as ultrasensitive sensing devices based on harnessing the non-Hermitian skin effect [75] by judiciously manipulating the boundary conditions.

As strongly correlated many-body states exhibit a rich variety of emergent phenomena, such as non-Abelian statistics, the study of their interplay with genuinely non-Hermitian effects as advanced here is likely to provide fertile ground for new fundamental discoveries.

K. Y. and E. J. B. acknowledge funding from the Swedish Research Council (VR) and the Knut and Alice Wallenberg Foundation. S. M. acknowledges funding from the Tsung-Dao Lee Institute.

[1] P. W. Anderson, The resonating valence bond state in La_2CuO_4 and superconductivity, Science **235**, 1196 (1987).
[2] L. Balents, Spin liquids in frustrated magnets, Nature (London) **464**, 199 (2010).
[3] L. Savary and L. Balents, Quantum spin liquids: A review, Rep. Prog. Phys. **80**, 016502 (2016).
[4] J. Knolle and R. Moessner, A field guide to spin liquids, Annu. Rev. Condens. Matter Phys. **10**, 451 (2019).
[5] C. Broholm, R. J. Cava, S. A. Kivelson, D. G. Nocera, M. R. Norman, and T. Senthil, Quantum spin liquids, Science **367**, eaay0668 (2020).
[6] A. Kitaev, Fault-tolerant quantum computation by anyons, Ann. Phys. (Amsterdam) **303**, 2 (2003).
[7] A. Kitaev, Anyons in an exactly solved model and beyond, Ann. Phys. (Amsterdam) **321**, 2 (2006), January Special Issue.
[8] M. A. Levin and X.-G. Wen, String-net condensation: A physical mechanism for topological phases, Phys. Rev. B **71**, 045110 (2005).
[9] H. Yao and S. A. Kivelson, Exact Chiral Spin Liquid with Non-Abelian Anyons, Phys. Rev. Lett. **99**, 247203 (2007).
[10] D. F. Schroeter, E. Kapit, R. Thomale, and M. Greiter, Spin Hamiltonian for which the Chiral Spin Liquid is the Exact Ground State, Phys. Rev. Lett. **99**, 097202 (2007).
[11] S. Mandal and N. Surendran, Exactly solvable Kitaev model in three dimensions, Phys. Rev. B **79**, 024426 (2009).
[12] V. Chua, H. Yao, and G. A. Fiete, Exact chiral spin liquid with stable spin Fermi surface on the kagome lattice, Phys. Rev. B **83**, 180412(R) (2011).
[13] S. C. Morampudi, C. von Keyserlingk, and F. Pollmann, Numerical study of a transition between $\mathbb{Z}_2$ topologically ordered phases, Phys. Rev. B **90**, 035117 (2014).
[14] O. Buerschaper, S. C. Morampudi, and F. Pollmann, Double semion phase in an exactly solvable quantum dimer model on the kagome lattice, Phys. Rev. B **90**, 195148 (2014).
[15] B. Horstmann, J. I. Cirac, and G. Giedke, Noise-driven dynamics and phase transitions in fermionic systems, Phys. Rev. A **87**, 012108 (2013).
[16] N. Matsumoto, K. Kawabata, Y. Ashida, S. Furukawa, and M. Ueda, Continuous Phase Transition without Gap Closing in Non-Hermitian Quantum Many-Body Systems, Phys. Rev. Lett. **125**, 260601 (2020).
[17] L. Xiao, K. Wang, X. Zhan, Z. Bian, K. Kawabata, M. Ueda, W. Yi, and P. Xue, Observation of Critical Phenomena in Parity-Time-Symmetric Quantum Dynamics, Phys. Rev. Lett. **123**, 230401 (2019).
[18] R. Hanai and P. B. Littlewood, Critical fluctuations at a many-body exceptional point, Phys. Rev. Research **2**, 033018 (2020).

[19] E. J. Bergholtz, J. C. Budich, and F. K. Kunst, Exceptional topology of non-Hermitian systems, arXiv:1912.10048 [Rev. Mod. Phys. (to be published)].
[20] Z. Gong, Y. Ashida, K. Kawabata, K. Takasan, S. Higashikawa, and M. Ueda, Topological Phases of Non-Hermitian Systems, Phys. Rev. X **8**, 031079 (2018).
[21] A. Cerjan, S. Huang, M. Wang, K. P. Chen, Y. Chong, and M. C. Rechtsman, Experimental realization of a Weyl exceptional ring, Nat. Photonics **13**, 623 (2019).
[22] H. Zhou, C. Peng, Y. Yoon, C. W. Hsu, K. A. Nelson, L. Fu, J. D. Joannopoulos, M. Soljačić, and B. Zhen, Observation of bulk Fermi arc and polarization half charge from paired exceptional points, Science **359**, 1009 (2018).
[23] S. Yao, F. Song, and Z. Wang, Non-Hermitian Chern Bands, Phys. Rev. Lett. **121**, 136802 (2018).
[24] J. C. Budich, J. Carlström, F. K. Kunst, and E. J. Bergholtz, Symmetry-protected nodal phases in non-Hermitian systems, Phys. Rev. B **99**, 041406(R) (2019).
[25] E. J. Bergholtz and J. C. Budich, Non-Hermitian Weyl physics in topological insulator ferromagnet junctions, Phys. Rev. Research **1**, 012003(R) (2019).
[26] X. Zhang, K. Ding, X. Zhou, J. Xu, and D. Jin, Experimental Observation of an Exceptional Surface in Synthetic Dimensions with Magnon Polaritons, Phys. Rev. Lett. **123**, 237202 (2019).
[27] K. Kawabata, K. Shiozaki, M. Ueda, and M. Sato, Symmetry and Topology in Non-Hermitian Physics, Phys. Rev. X **9**, 041015 (2019).
[28] T. E. Lee, Anomalous Edge State in a Non-Hermitian Lattice, Phys. Rev. Lett. **116**, 133903 (2016).
[29] M. Berry, Physics of nonHermitian degeneracies, Czech. J. Phys. **54**, 1039 (2004).
[30] K. Ding, G. Ma, M. Xiao, Z. Q. Zhang, and C. T. Chan, Emergence, Coalescence, and Topological Properties of Multiple Exceptional Points and their Experimental Realization, Phys. Rev. X **6**, 021007 (2016).
[31] J.-H. Park, A. Ndao, W. Cai, L. Hsu, A. Kodigala, T. Lepetit, Y.-H. Lo, and B. Kanté, Symmetry-breaking-induced plasmonic exceptional points and nanoscale sensing, Nat. Phys. **16**, 462 (2020).
[32] M.-A. Miri and A. Alù, Exceptional points in optics and photonics, Science **363**, eaar7709 (2019).
[33] S. Yao and Z. Wang, Edge States and Topological Invariants of Non-Hermitian Systems, Phys. Rev. Lett. **121**, 086803 (2018).
[34] F. K. Kunst, E. Edvardsson, J. C. Budich, and E. J. Bergholtz, Biorthogonal Bulk-Boundary Correspondence in Non-Hermitian Systems, Phys. Rev. Lett. **121**, 026808 (2018).
[35] Y. Xiong, Why does bulk boundary correspondence fail in some non-Hermitian topological models, J. Phys. Commun. **2**, 035043 (2018).
[36] L. Xiao, T. Deng, K. Wang, G. Zhu, Z. Wang, W. Yi, and P. Xue, Non-Hermitian bulk–boundary correspondence in quantum dynamics, Nat. Phys. **16**, 761 (2020).
[37] H. Schomerus, Nonreciprocal response theory of non-Hermitian mechanical metamaterials: Response phase transition from the skin effect of zero modes, Phys. Rev. Research **2**, 013058 (2020).
[38] A. Ghatak, M. Brandenbourger, J. van Wezel, and C. Coulais, Observation of non-Hermitian topology and its bulk-edge correspondence, Proc. Natl. Acad. Sci. U.S.A. **117**, 29561 (2020).
[39] T. Helbig, T. Hofmann, S. Imhof, M. Abdelghany, T. Kiessling, L. Molenkamp, C. Lee, A. Szameit, M. Greiter, and R. Thomale, Generalized bulk–boundary correspondence in non-Hermitian topolectrical circuits, Nat. Phys. **16**, 747 (2020).
[40] T. Yoshida, R. Peters, N. Kawakami, and Y. Hatsugai, Symmetry-protected exceptional rings in two-dimensional correlated systems with chiral symmetry, Phys. Rev. B **99**, 121101(R) (2019).
[41] T. Yoshida, K. Kudo, and Y. Hatsugai, Non-Hermitian fractional quantum Hall states, Sci. Rep. **9**, 1 (2019).
[42] C. H. Lee, Many-body topological and skin states without open boundaries, arXiv:2006.01182.
[43] T. Liu, J. J. He, T. Yoshida, Z.-L. Xiang, and F. Nori, Non-Hermitian topological Mott insulators in one-dimensional fermionic superlattices, Phys. Rev. B **102**, 235151 (2020).
[44] J. Carlström, Correlations in non-Hermitian systems and diagram techniques for the steady state, Phys. Rev. Research **2**, 013078 (2020).
[45] H. Shackleton and M. S. Scheurer, Protection of parity-time symmetry in topological many-body systems: Non-Hermitian toric code and fracton models, Phys. Rev. Research **2**, 033022 (2020).
[46] T. Yoshida, K. Kudo, H. Katsura, and Y. Hatsugai, Fate of fractional quantum Hall states in open quantum systems: Characterization of correlated topological states for the full Liouvillian, Phys. Rev. Research **2**, 033428 (2020).
[47] N. P. Armitage, E. J. Mele, and A. Vishwanath, Weyl and dirac semimetals in three-dimensional solids, Rev. Mod. Phys. **90**, 015001 (2018).
[48] G. Lindblad, On the generators of quantum dynamical semigroups, Commun. Math. Phys. **48**, 119 (1976).
[49] R. Dum, P. Zoller, and H. Ritsch, Monte carlo simulation of the atomic master equation for spontaneous emission, Phys. Rev. A **45**, 4879 (1992).
[50] K. Mølmer, Y. Castin, and J. Dalibard, Monte Carlo wavefunction method in quantum optics, J. Opt. Soc. Am. B **10**, 524 (1993).
[51] M. B. Plenio and P. L. Knight, The quantum-jump approach to dissipative dynamics in quantum optics, Rev. Mod. Phys. **70**, 101 (1998).
[52] A. J. Daley, Quantum trajectories and open many-body quantum systems, Adv. Phys. **63**, 77 (2014).
[53] T. E. Lee and C.-K. Chan, Heralded Magnetism in Non-Hermitian Atomic Systems, Phys. Rev. X **4**, 041001 (2014).
[54] Y. Ashida, S. Furukawa, and M. Ueda, Quantum critical behavior influenced by measurement backaction in ultracold gases, Phys. Rev. A **94**, 053615 (2016).
[55] M. Nakagawa, N. Tsuji, N. Kawakami, and M. Ueda, Dynamical Sign Reversal of Magnetic Correlations in Dissipative Hubbard Models, Phys. Rev. Lett. **124**, 147203 (2020).
[56] N. Shibata and H. Katsura, Dissipative spin chain as a non-Hermitian Kitaev ladder, Phys. Rev. B **99**, 174303 (2019).
[57] E. H. Lieb, Flux Phase of the Half-Filled Band, Phys. Rev. Lett. **73**, 2158 (1994).
[58] See Supplemental Material at http://link.aps.org/supplemental/10.1103/PhysRevLett.126.077201 for a de-

tailed calculation of the band-touching points and OBC solutions.

[59] F. K. Kunst and V. Dwivedi, Non-Hermitian systems and topology: A transfer-matrix perspective, Phys. Rev. B **99**, 245116 (2019).

[60] J. Knolle, D. L. Kovrizhin, J. T. Chalker, and R. Moessner, Dynamics of a Two-Dimensional Quantum Spin Liquid: Signatures of Emergent Majorana Fermions and Fluxes, Phys. Rev. Lett. **112**, 207203 (2014).

[61] S. C. Morampudi, A. M. Turner, F. Pollmann, and F. Wilczek, Statistics of Fractionalized Excitations through Threshold Spectroscopy, Phys. Rev. Lett. **118**, 227201 (2017).

[62] Y. Werman, S. Chatterjee, S. C. Morampudi, and E. Berg, Signatures of Fractionalization in Spin Liquids from Interlayer Thermal Transport, Phys. Rev. X **8**, 031064 (2018).

[63] S. C. Morampudi, F. Wilczek, and C. R. Laumann, Spectroscopy of Spinons in Coulomb Quantum Spin Liquids, Phys. Rev. Lett. **124**, 097204 (2020).

[64] L.-M. Duan, E. Demler, and M. D. Lukin, Controlling Spin Exchange Interactions of Ultracold Atoms in Optical Lattices, Phys. Rev. Lett. **91**, 090402 (2003).

[65] A. Micheli, G. Pupillo, H. P. Büchler, and P. Zoller, Cold polar molecules in two-dimensional traps: Tailoring interactions with external fields for novel quantum phases, Phys. Rev. A **76**, 043604 (2007).

[66] G. Jackeli and G. Khaliullin, Mott Insulators in the Strong Spin-Orbit Coupling Limit: From Heisenberg to a Quantum Compass and Kitaev Models, Phys. Rev. Lett. **102**, 017205 (2009).

[67] R. Schmied, J. H. Wesenberg, and D. Leibfried, Quantum simulation of the hexagonal Kitaev model with trapped ions, New J. Phys. **13**, 115011 (2011).

[68] J. Q. You, X.-F. Shi, X. Hu, and F. Nori, Quantum emulation of a spin system with topologically protected ground states using superconducting quantum circuits, Phys. Rev. B **81**, 014505 (2010).

[69] A. V. Gorshkov, K. R. Hazzard, and A. M. Rey, Kitaev honeycomb and other exotic spin models with polar molecules, Mol. Phys. **111**, 1908 (2013).

[70] T. Yoshida, R. Peters, N. Kawakami, and Y. Hatsugai, Exceptional band touching for strongly correlated systems in equilibrium, Prog. Theor. Exp. Phys. **2020**, 12A109 (2020).

[71] M. Naghiloo, M. Abbasi, Y. N. Joglekar, and K. Murch, Quantum state tomography across the exceptional point in a single dissipative qubit, Nat. Phys. **15**, 1232 (2019).

[72] I. Bloch, J. Dalibard, and W. Zwerger, Many-body physics with ultracold gases, Rev. Mod. Phys. **80**, 885 (2008).

[73] J.-F. Riou, A. Reinhard, L. A. Zundel, and D. S. Weiss, Spontaneous-emission-induced transition rates between atomic states in optical lattices, Phys. Rev. A **86**, 033412 (2012).

[74] S. Friebel, C. D'Andrea, J. Walz, M. Weitz, and T. W. Hänsch, CO_2-laser optical lattice with cold rubidium atoms, Phys. Rev. A **57**, R20(R) (1998).

[75] J. C. Budich and E. J. Bergholtz, Non-Hermitian Topological Sensors, Phys. Rev. Lett. **125**, 180403 (2020).